

# Pyrolysis of methylcyclohexane: kinetics and modelling

Kamal K. Pant, Deepak Kunzru \*

Department of Chemical Engineering, Indian Institute of Technology, Kanpur 208016, India

Received 24 September 1996; revised 7 February 1997; accepted 19 February 1997

## Abstract

Steam pyrolysis of methylcyclohexane has been investigated in a tubular reactor at atmospheric pressure in the temperature range 953–1073 K. Using non-linear regression, the overall decomposition was found to be approximately first-order with a pre-exponential factor and activation energy of  $1.71 \times 10^{11} \text{ s}^{-1}$  and  $209.0 \text{ kJ mol}^{-1}$ , respectively. The experimental product yields and conversion could be satisfactorily simulated using a molecular model consisting of an overall primary reaction and twenty-four secondary reactions. © 1997 Elsevier Science S.A.

**Keywords:** Pyrolysis modelling; Methylcyclohexane; Thermal cracking; Kinetics

## 1. List of symbols

$A_c$	cross-sectional area of reactor/ $\text{m}^2$
$C_A$	concentration of methylcyclohexane/ $\text{mol m}^{-3}$
$E$	activation energy/ $\text{J mol}^{-1}$
$F_{A_0}$	molar feed rate of methylcyclohexane/ $\text{mol s}^{-1}$
$F_{S_0}$	molar feed rate of steam/ $\text{mol s}^{-1}$
$k_0$	pre-exponential factor
$k_0^*$	reparameterized pre-exponential factor, defined in Eq. (5)
$l$	reactor length/m
$n$	overall reaction order
$P$	total pressure/Pa
$R$	gas constant/ $\text{J mol}^{-1}\text{K}^{-1}$
$T$	reactor temperature/K
$X_A$	conversion of methylcyclohexane

### Greek symbols

$\delta$	molar dilution ratio, mol of steam per mol of methylcyclohexane fed
$\epsilon$	expansion factor
$\nu$	stoichiometric coefficient, moles of total product per mol of methylcyclohexane cracked

## 2. Introduction

Light olefins are commonly manufactured by steam pyrolysis of hydrocarbons such as ethane, propane or naphtha. In

addition to the process variables such as reactor temperature, hydrocarbon partial pressure and residence time, the product yields significantly depend on the nature of the feedstock. In order to optimize the pyrolysis process, it is necessary to study the pyrolysis of individual hydrocarbons as well as mixtures of hydrocarbons. Although extensive literature has been published on the experimental and modelling aspects of *n*-paraffin pyrolysis, very little information is available on the pyrolysis of naphthenes. Most of the work has concentrated on cyclohexane pyrolysis. In the only study available in the published literature on methylcyclohexane pyrolysis, Bajus et al. [1] investigated the thermal decomposition of methylcyclohexane in the presence of steam in a flow reactor in the temperature range of 953–1063 K. The overall reaction was first-order with an activation energy of  $201.3 \text{ kJ mol}^{-1}$ . No model was proposed by them to explain the experimental product yields.

The objective of this study was to investigate the effect of temperature and space time on the product yields during methylcyclohexane pyrolysis over a wide range of conversion. Another objective was to develop a kinetic model based on the observed product yields.

## 3. Experimental

The pyrolysis runs were conducted in an annular tubular reactor and the experimental apparatus was the same as used for an earlier study on catalytic pyrolysis [2]. The reactor (19 mm i.d.  $\times$  25 mm o.d.) was constructed of stainless steel

\* Corresponding author. Fax +91 512 250260 or 250007.

and heated in a three-zone furnace. The heated reactor length was 600 mm. Preheated methylcyclohexane and steam were fed to the reactor by micropumps. The flow rates of water and methylcyclohexane could be varied in the range of 0 to 15 ml min<sup>-1</sup>. To reduce the coke deposition on the walls of the reactor, 200 ppm carbon disulphide was added to the hydrocarbon feed. During the course of a run, the total condensed water and organic liquid, together with the volume and composition of the non-condensable gases, was measured at regular intervals. At the completion of a run, the reactor was flushed with steam for 1 h, and then the reactor was decoked with air.

The non-condensable gases, which mainly consisted of C<sub>1</sub>–C<sub>4</sub> hydrocarbons and carbon oxides, were analysed by gas chromatography using three columns as detailed elsewhere [3]. The liquid products were analysed on a capillary column (Petrocol DH column; i.d., 0.25 mm; length, 100 m) using FID and nitrogen as the carrier gas.

#### 4. Results and discussion

The pyrolysis of methylcyclohexane was conducted in the presence of steam at atmospheric pressure for various temperatures and space times. The experiments covered the following range of variables: temperature, 953–1073 K; methylcyclohexane flow rate, 0.5 to 2.5 g min<sup>-1</sup>, and thus a space time of 0.1 to 0.7 s. The inlet molar ratio of steam to methylcyclohexane,  $\delta$ , was kept fixed at 13.6 for all the runs.

##### 4.1. Kinetic analysis

Due to the inevitable temperature profile in a tubular reactor, the kinetics of hydrocarbon pyrolysis is usually determined by calculating the equivalent reactor volume using a pseudo-isothermal analysis. This technique utilizes the measured temperature profile to convert the data to isothermal conditions at a chosen reference temperature [4,5]. However, in this study, the kinetic constants and the overall reaction order have been determined using non-linear optimization in which the actual temperature profile for each run was considered.

The variation of methylcyclohexane conversion with space time at different reference temperatures is shown in Fig. 1. To prevent cracking in the preheater, the feed inlet temperature was limited to 823 K, and there were significant axial gradients at the reactor inlet and exit. Depending on the set temperature, the axial temperature gradient at the inlet was 15–20 K cm<sup>-1</sup>, and at the exit 10–12 K cm<sup>-1</sup>. However, in the central portion of the reactor, which extended from 20 to 40 cm from the reactor inlet, there were no axial gradients. Due to this axial temperature profile, a unique temperature for a run is not defined and the reference temperature for a run was taken to be equal to the temperature in the central isothermal zone of the reactor.

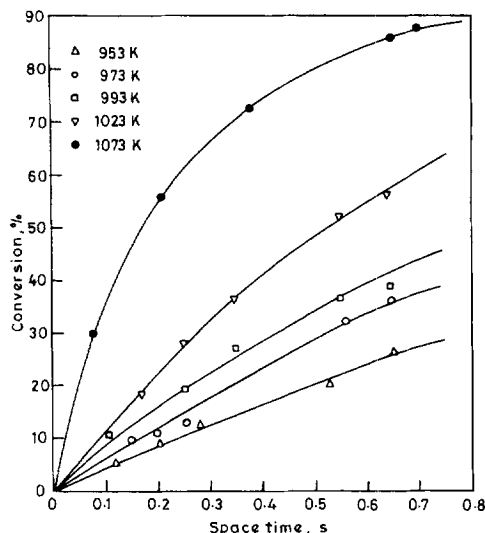


Fig. 1. Variation of the conversion of methylcyclohexane with space time at different temperatures.

It should be emphasized that neither the reference temperature nor the calculated equivalent reactor volume have been used for evaluating the kinetic constants.

Making a mass balance on a differential element of the reactor, we obtain

$$\frac{F_{A0}}{A_c} \frac{dX_A}{dl} = k_o \exp\left(\frac{-E}{RT}\right) C_A^n \quad (1)$$

where

$$C_A = \frac{F_{A0}}{(F_{A0} + F_{S0})} \frac{(1 - X_A)}{(1 + \epsilon X_A)} \frac{P}{RT} \quad (2)$$

and

$$\epsilon = \frac{\nu - 1}{1 + \delta} \quad (3)$$

Excluding hydrogen, the moles of product formed per mole of methylcyclohexane cracked were evaluated from the experimental data and varied from 2.1 at low conversions to 2.8 at high conversions. Hydrogen in the product gases was not determined quantitatively and to evaluate  $\nu$  it was assumed that 0.43 moles of H<sub>2</sub> are formed per mole of methylcyclohexane decomposed [1]. Due to the high steam dilution, the calculated conversions were not sensitive to the value of  $\nu$ .

The kinetic constants were determined by minimizing the sum of squares of the deviation between the calculated and the experimental conversions for all the runs by varying  $k_o$ ,  $E$  and  $n$ . Due to the strong correlation between  $k_o$  and  $E$ , Eq. (1) was reparameterized as

$$\frac{dX_A}{dl} = \frac{A_c}{F_{A0}} k_o^* \exp\left[-\frac{E}{R} \left(\frac{1}{T} - \frac{1}{T^*}\right)\right] C_A^n \quad (4)$$

where

$$k_o^* = k_o \exp\left(\frac{-E}{RT^*}\right) \quad (5)$$

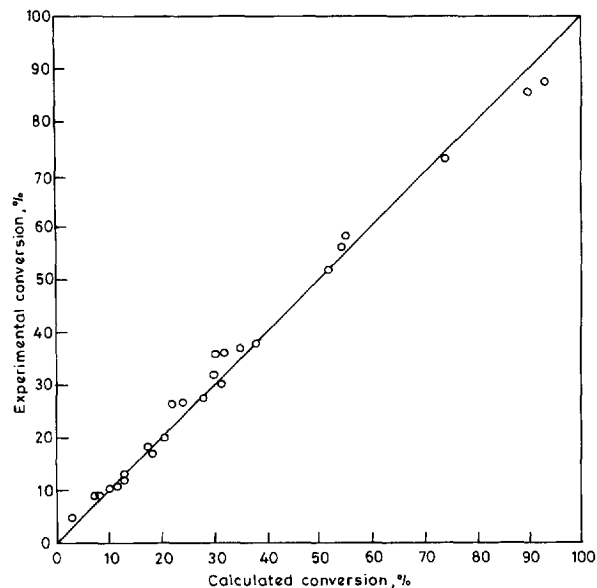


Fig. 2. Comparison between experimental and calculated conversions.

where  $T^*$  was taken to be 973 K. Eq. (4) was numerically integrated using a fourth-order Runge–Kutta–Gill algorithm. The axial temperature profile was measured at 3 cm intervals and, for each run, the profile was fitted to a fourth-order polynomial for use in the numerical integration. The objective function was minimized using the Box-complex algorithm. Based on the minimization,  $k_0$ ,  $E$  and  $n$  were  $2.21 \times 10^{11} \text{ s}^{-1} (\text{m}^3 \text{ mol}^{-1})^{0.06}$ ,  $211.0 \text{ kJ mol}^{-1}$  and 1.06, respectively. For the subsequent analysis, the order was taken to be unity and the pre-exponential factor and activation energy, recalculated by minimization of the objective function, were  $1.71 \times 10^{11} \text{ s}^{-1}$  and  $209.0 \text{ kJ mol}^{-1}$ , respectively. The comparison between the experimental and calculated conversions is shown in Fig. 2. As can be seen from Fig. 2, the difference between the calculated and experimental conversions is small, even for high conversions. The activation energy and frequency factor obtained in this study are in good agreement with the values of  $201.3 \text{ kJ mol}^{-1}$  and  $0.532 \times 10^{11} \text{ s}^{-1}$  reported by Bajus et al. [1]. No other data on the kinetics of methylcyclohexane pyrolysis have been published. Since the alkyl group can be easily cleaved, the rate of decomposition of methylcyclohexane is significantly higher than that of cyclohexane [6,7]. For instance, in their model for cyclohexane pyrolysis, Aribike et al. [7] proposed that cyclohexane can decompose by three parallel routes having activation energies of 70.5, 67.5 and 67.0  $\text{kcal mol}^{-1}$ . Based on their pre-exponential factors, the overall rate constant for cyclohexane decomposition at 973 K is  $0.15 \text{ s}^{-1}$  compared to the value of  $1.0 \text{ s}^{-1}$  for methylcyclohexane. On the other hand, under identical conditions the rate of decomposition of methylcyclohexane is approximately one half the rate of decomposition of *n*-heptane [8].

#### 4.2. Product distribution

The effect of temperature and space time on the product yields and selectivities was investigated. The main products

were methane, ethylene, propylene, 1,3-butadiene, cyclohexene, isoprene, benzene and toluene. In addition, small amounts of propane, 1-butene, 3-methylbutene-1, methylcyclohexenes, pentadienes, 2-heptene, cyclohexane, methylcyclopentadienes, cyclohexadienes and  $\text{C}_8$  aromatics were also detected. Carbon oxides were detected only at 1073 K and high conversions. (At 1073 K and a conversion of 87.5%, the CO and  $\text{CO}_2$  yields were respectively 1.2 and 6.5 moles per 100 moles methylcyclohexane decomposed.) The variation in product selectivities (moles product per 100 moles methylcyclohexane decomposed) with conversion for the main products at different reference temperatures is shown in Figs. 3–6, whereas the detailed product selectivities for some selected runs are shown in Table 1. As can be seen from these figures for a fixed conversion, there was no noticeable effect of temperature on selectivities. At all conditions, ethylene was the main product and its yield varied from 0.8 wt% feed at low conversions to 24.3 wt% feed at the highest conversion (87.5%) studied. Depending on the primary and secondary reactions, the selectivities of the various products either increased, decreased or showed a maximum with increasing conversion. The selectivities of methane (Fig. 4) and benzene (Fig. 6) increased monotonically with conversion, showing a steeper rise at high conversions, whereas the ethylene selectivity (Fig. 3) tended to level off at high conversions. The selectivities of propylene and 1,3-butadiene showed maxima, whereas the selectivity of isoprene was nearly constant up to a conversion of 30% and decreased at higher conversions (Figs. 3–5). The selectivities of cyclohexene (Fig. 5) and toluene (Fig. 6) decreased with increasing conversion, indicating that these are formed in the primary step and react further at high conversions. Similarly, as can be deduced from Table 1, methylcyclohexenes were also obtained as primary products. The selectivities of 1, *trans*-3-pentadiene, 1, *cis*-3-pentadiene, 1,4-pentadiene, 1,3-cyclohexadiene, 1-methylcyclopentene and 1,3-cyclopentadiene were negligible at low conversions (Table 1) which suggests that these were formed by secondary reactions. The trend of some of the product selectivities with conversion is at variance with the trends reported by Bajus et al. [1]. At 973 K, they indicated the product selectivities of ethylene, propylene and 1,3-butadiene to be zero at 0% conversion, whereas finite values were obtained in this study. Moreover, they did not report any decrease in the selectivities of propylene, 1,3-butadiene or isoprene with increasing conversion. This could be due to the limited range of conversion investigated in their study.

The product distribution can be qualitatively explained by considering the possible initiation routes for the thermal decomposition of methylcyclohexane and the subsequent reactions of the free radicals thus formed. The initiation of methylcyclohexane decomposition can occur by: (i) removal of a methyl radical to form  $c\text{-C}_6\text{H}_{11}$ ; (ii) formation of methylcyclohexyl radicals by removal of  $\text{H}\cdot$  from the 1, 2, 3, or 4 positions; or (iii) cleavage of one of the C–C bonds of the ring to form different isomers of  $\text{C}_7$  biradicals. In initiation

Table 1  
Product distribution in pyrolysis of methylcyclohexane (moles of product formed/100 moles of methylcyclohexane cracked)

	Reference temperature/K									
	953	953	973	973	993	993	1023	1023	1073	1073
	Conversion %									
	5.1	26.5	9.4	36.0	10.2	38.3	17.8	58.0	72.5	85.5
Methane	48.0	59.4	48.2	58.0	53.0	61.3	52.5	75.4	79.8	91.1
Ethane	3.2	5.3	3.9	4.4	4.0	4.8	3.0	6.3	3.4	6.3
Ethylene	68.5	80.4	70.5	82.8	71.7	83.3	71.7	91.5	87.8	96.7
Propane	tr	0.4	tr	0.2	tr	0.2	0.3	0.3	0.2	0.2
Propylene	29.7	43.6	32.8	32.5	32.9	42.7	35.4	46.0	38.2	35.8
Butene-1	tr	2.5	0.2	1.9	0.8	2.1	0.7	1.3	1.3	0.5
1,3-Butadiene	18.7	25.5	22.0	26.1	24.0	30.1	22.1	35.5	28.4	18.1
3-Methylbutene-1	0.9	1.6	2.3	2.3	tr	tr	1.0	0.6	0.4	0.2
1,4-Pentadiene	0.0	1.2	2.5	2.5	3.1	1.5	3.8	1.9	2.0	1.6
Isoprene	12.5	4.5	6.8	5.4	10.0	9.2	6.0	4.5	5.0	1.6
1,trans-3-pentadiene	2.0	2.5	2.9	1.2	2.8	1.4	2.9	1.6	2.2	2.1
1,cis-3-pentadiene	0.9	2.1	0.9	0.5	2.7	1.9	2.4	1.4	0.6	0.3
Cyclohexene	15.0	4.6	10.6	4.8	9.9	7.5	6.8	3.3	3.1	2.9
Benzene	1.8	2.4	2.1	3.9	3.7	4.5	2.4	6.2	9.7	12.6
2-Heptene	0.0	0.7	0.0	0.0	0.6	1.1	0.0	0.0	0.0	0.0
Methylcyclopentadiene	0.0	0.0	1.0	0.8	0.6	0.5	2.3	1.1	0.5	0.2
Toluene	6.2	2.6	5.5	2.8	4.5	2.5	2.9	0.9	1.9	1.1
Cyclohexane	0.0	0.0	1.9	tr	tr	0.7	1.3	1.0	0.1	0.1
3-Methylcyclohexene + 4-methylcyclohexene	3.2	1.8	1.1	1.0	1.0	0.6	1.2	0.5	0.0	0.0
1-Methylcyclohexene	2.5	1.9	2.0	1.5	2.0	1.5	1.3	0.3	0.2	0.1
1,3-Cyclopentadiene	0.0	0.0	0.0	0.0	0.0	1.0	1.3	0.3	0.2	0.1
1-Methylcyclopentene	0.0	0.0	0.0	0.0	0.0	0.0	0.0	0.6	0.2	0.1
1,3-Cyclohexadiene	0.0	0.0	0.0	0.0	0.0	0.0	0.0	0.8	0.2	0.1
Others	0.0	0.9	0.0	1.8	0.0	1.3	0.0	0.6	0.9	1.8

tr = trace.

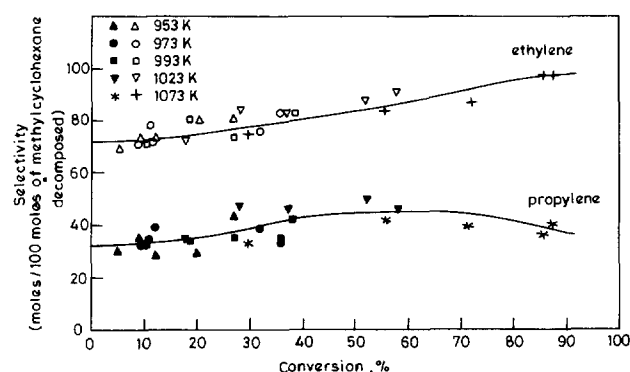
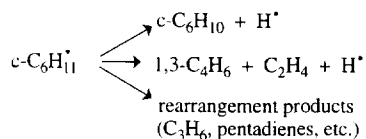
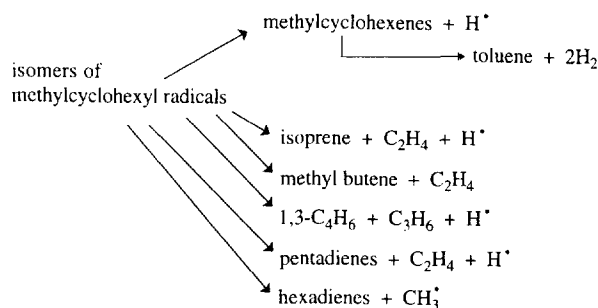


Fig. 3. Variation of ethylene and propylene selectivities with conversion.

according to (ii), removal of  $H\cdot$  from the 1 position is most likely but due to the fast isomerization, the different methylcyclohexyl radicals will be at equilibrium. Considering the bond energies, the most favoured initiation route is the formation of cyclohexyl and methyl radicals [1]. The cyclohexyl radical thus formed can decompose in various ways [9] as follows:



The methylcyclohexyl radicals, formed by initiation and isomerization, can give methylcyclohexenes by removal of  $H\cdot$  or form various products by ring opening and  $\beta$ -scission, as shown below:



The  $C_7$  biradicals formed in the initiation step can isomerize to heptenes or decompose by  $\beta$ -scission of a  $C-C$  bond to yield  $C_2H_4$ , isoprene, 1,3- $C_4H_6$ , methylbutene,  $C_3H_6$ , pentadienes and hexadienes. In addition, as suggested by Bajus et al. [1], heptadienes can be formed by splitting of  $C_7$  biradicals at the  $C-H$  bond.

#### 4.3. Model development

Fundamental studies carried out by several groups of workers have established the general free radical nature of the

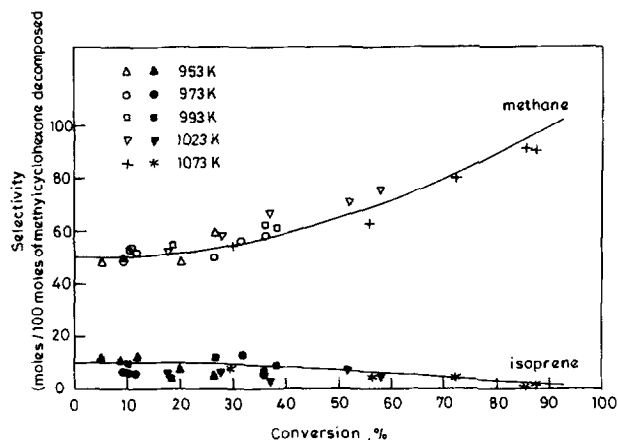


Fig. 4. Variation of methane and isoprene selectivities with conversion.

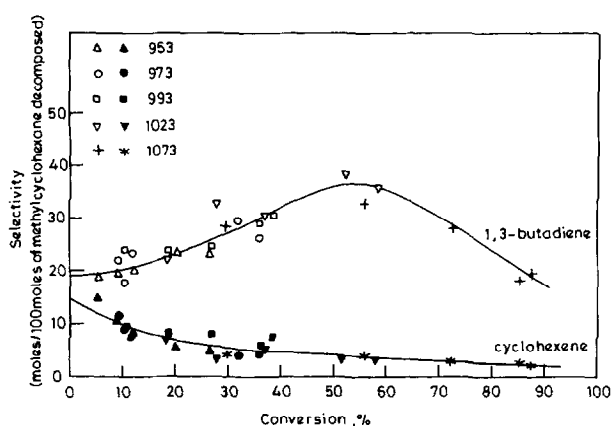


Fig. 5. Variation of 1,3-butadiene and cyclohexene selectivities with conversion.

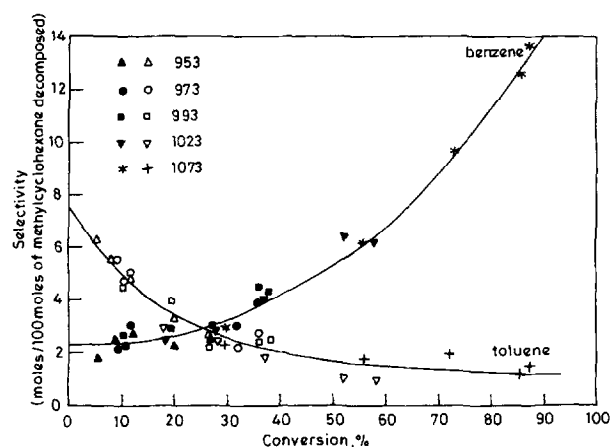
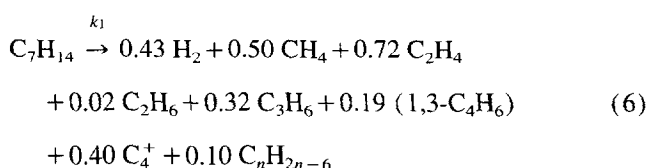


Fig. 6. Variation of benzene and toluene selectivities with conversion.

pyrolysis reactions. However, there is still disagreement among different workers regarding the elementary radical reactions to be included for a particular hydrocarbon, as well as on the value of the kinetic constants for the same elementary reaction [10–12]. Due to the incomplete knowledge of the kinetics of free radical reactions, especially for radicals containing more than four carbon atoms, a mechanistic model for methylcyclohexane pyrolysis was not attempted and a molecular model has been developed to simulate the product

distribution. In molecular models, the pyrolysis is generally represented by an overall primary reaction followed by a set of secondary reactions between the primary products. Such an approach has been successfully applied for modelling the pyrolysis of ethane, propane, butane and their mixtures [13,14] and extended to  $C_8$  normal and branched paraffins [12]. Molecular models have also been developed for pyrolysis of naphtha [5] and atmospheric gas oil [15].

Based on the kinetic analysis, the overall order for the primary reaction was taken to be first order and the initial selectivities were assumed to be independent of temperature. Except for  $H_2$ , the initial selectivities were obtained experimentally. To simplify the model, the non-aromatic products heavier than  $C_4$  were lumped together as  $C_4^+$  and the aromatic fraction as  $C_nH_{2n-6}$ . The  $C_4^+$  fraction mainly consisted of olefins and cycloolefins, whereas the main components of the aromatic fraction were benzene and toluene. The average carbon number of the  $C_4^+$  and  $C_nH_{2n-6}$  fractions were estimated to be 6.5 and 6.8, respectively. Thus, the primary reaction was represented as



A large number of secondary reactions can take place between the various primary products. An attempt has been made to include the important secondary reactions that will account for the major products obtained during the pyrolysis of methylcyclohexane. Kumar and Kunzru [5] proposed a set of secondary reactions which was found to model satisfactorily the product yields obtained during the pyrolysis of naphtha, gas oil and kerosene. A similar set of secondary reactions have been used to model gas oil pyrolysis [15]. In their study of computer generation of reaction schemes for thermal cracking, Hillewaert et al. [16] also reported that their set of secondary reactions was more or less independent of the feed composition. They, however, did not report the set of secondary reactions used.

To model the pyrolysis of methylcyclohexane, the set of secondary reactions proposed for naphtha pyrolysis [5] was first tried. However, with this reaction scheme, the predicted ethylene and propylene yields were lower whereas the  $C_4^+$  yields were higher than the experimental yields. To improve the match between the experimental and calculated yields, three additional secondary reactions, which account for the decomposition of  $C_4^+$  components into lighter components, were appended to the secondary scheme for naphtha pyrolysis. These reactions were



Table 2  
Reaction scheme for the pyrolysis of methylcyclohexane

Reaction	Pre-exponential factor/ $s^{-1}$ or $m^3 \text{ mol}^{-1} s^{-1}$	Activation energy/ $\text{kJ mol}^{-1}$	Source
(1) $C_7H_{14} \rightarrow 0.43H_2 + 0.50CH_4 + 0.72C_2H_4 + 0.02C_2H_6 + 0.32C_3H_6 + 0.19(1,3-C_4H_6) + 0.40C_4^+ + 0.10C_nH_{2n-6}$	$1.71 \times 10^{11}$	209.0	This work
(2) $C_2H_6 \rightleftharpoons C_2H_4 + H_2$	$4.65 \times 10^{13}$	273.0	[14]
(3) $C_3H_6 \rightleftharpoons C_2H_2 + CH_4$	$7.28 \times 10^{12}$	273.5	[5]
(4) $C_2H_2 + C_2H_4 \rightarrow C_4H_6$	$1.03 \times 10^{9a}$	172.7	[14]
(5) $2C_2H_6 \rightarrow C_3H_8 + CH_4$	$3.75 \times 10^{12}$	273.1	[14]
(6) $C_2H_4 + C_2H_6 \rightarrow C_3H_6 + CH_4$	$7.08 \times 10^{10a}$	253.0	[14]
(7) $C_3H_8 \rightleftharpoons C_3H_6 + H_2$	$5.89 \times 10^{10}$	214.7	[14]
(8) $C_3H_8 \rightarrow C_2H_4 + CH_4$	$4.69 \times 10^{10}$	211.8	[14]
(9) $C_3H_8 + C_2H_4 \rightarrow C_2H_6 + C_3H_6$	$2.54 \times 10^{10a}$	247.2	[14]
(10) $2C_3H_6 \rightarrow 3C_2H_4$	$1.2 \times 10^{12}$	244.9	a
(11) $2C_3H_6 \rightarrow 0.3C_nH_{2n-6} + 0.14C_4^+ + 3CH_4$	$1.42 \times 10^{11}$	228.1	a
(12) $C_3H_6 + C_2H_6 \rightarrow C_4H_8 + CH_4$	$1.0 \times 10^{11a}$	251.2	[14]
(13) $n-C_4H_{10} \rightarrow C_3H_6 + CH_4$	$7.0 \times 10^{12}$	249.7	[14]
(14) $n-C_4H_{10} \rightarrow 2C_2H_4 + H_2$	$7.0 \times 10^{14}$	295.9	[14]
(15) $n-C_4H_{10} \rightarrow C_2H_4 + C_2H_6$	$4.1 \times 10^{12}$	256.6	[14]
(16) $n-C_4H_{10} \rightleftharpoons C_4H_8 + H_2$	$1.64 \times 10^{12}$	261.0	[14]
(17) $1-C_4H_8 \rightarrow 0.41C_nH_{2n-6} + 0.19C_4^+$	$2.08 \times 10^{11}$	212.2	[5]
(18) $1-C_4H_8 \rightleftharpoons C_4H_6 + H_2$	$1.0 \times 10^{10}$	209.3	[5]
(19) $C_4H_6 + C_2H_4 \rightarrow B + 2H_2$	$8.38 \times 10^{6a}$	144.7	[5]
(20) $C_4H_6 + C_3H_6 \rightarrow T + 2H_2$	$9.74 \times 10^{5a}$	149.2	[5]
(21) $C_4H_6 + 1-C_4H_8 \rightarrow EB + 2H_2$	$6.4 \times 10^{11a}$	242.4	[5]
(22) $2C_4H_6 \rightarrow ST + 2H_2$	$1.5 \times 10^{6a}$	124.3	[5]
(23) $C_4^+ \rightarrow 1.3C_2H_4 + 1.3C_3H_6$	$4.6 \times 10^{11}$	221.5	a
(24) $C_4^+ \rightarrow 1.3CH_4 + 1.3C_4H_8$	$1.1 \times 10^{10}$	190.5	a
(25) $C_4^+ + H_2 \rightarrow 1.3(1-C_4H_8) + 1.3CH_4$	$4.0 \times 10^{11}$	230.2	a

<sup>a</sup> Units:  $m^3 \text{ mol}^{-1} s^{-1}$ .

B: benzene; T: toluene; EB: ethyl benzene, ST; styrene.

a: estimated by authors.

For reactions (7)–(9), a stoichiometric coefficient of 1.3 was calculated from the carbon balance.

The reaction scheme consists of a primary reaction and a set of twenty-four secondary reactions (Table 2). The equilibrium constants for the reversible reactions (reactions (2), (3), (7), (16) and (18) of Table 2) were calculated by standard procedures and checked with published values. With this reaction scheme, the continuity equations for the 14 components were solved using a fourth-order Runge–Kutta–Gill method. In the numerical integration, the actual temperature profile for each run was used. The experimental and calculated product yields were compared, and the kinetic constants of some of the secondary reactions adjusted to reduce the error. The final values of the pre-exponential factor and activation energy for each reaction are shown in Table 2. Compared to the set of secondary reactions for naphtha pyrolysis [5], in addition to the three reactions for  $C_4^+$  (reactions (23)–(25), Table 2), the pre-exponential factors and activation energies of reactions (10) and (11) had to be modified to improve the match between the calculated and experimental yields of ethylene and propylene. The kinetic constants for the remaining nineteen secondary reactions are the same as for naphtha pyrolysis.

The simulation model developed was used to compare the experimental and predicted yields. At a fixed conversion, the

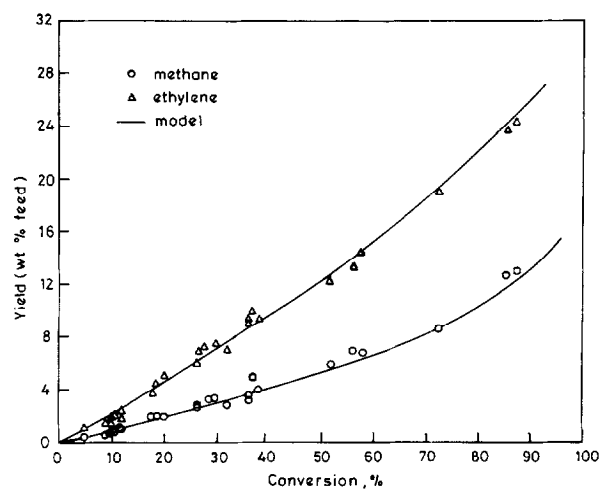


Fig. 7. Comparison between predicted and experimental yields of methane and ethylene.

effect of temperature on individual product selectivities was negligible, and, therefore, the experimental and calculated yields obtained at different temperatures have been shown on single plots ( Figs. 7–9). As can be seen from these figures, the predicted and experimental yields of  $CH_4$ ,  $C_3H_6$ ,  $C_4^+$  and aromatics are in good agreement for the whole conversion range, whereas the calculated and experimental yields of

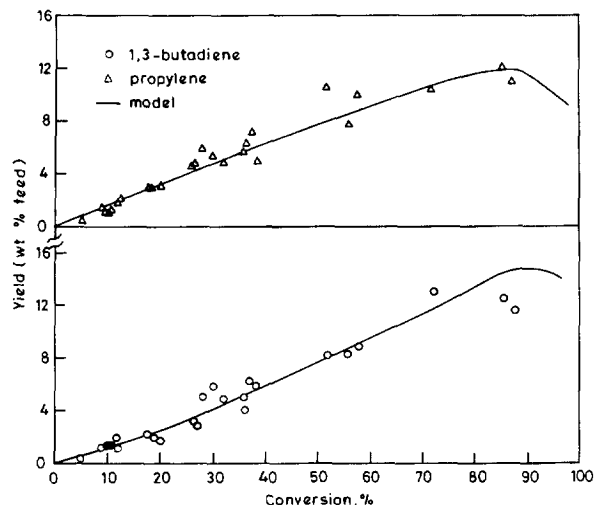


Fig. 8. Comparison between predicted and experimental yields of 1,3-butadiene and propylene.

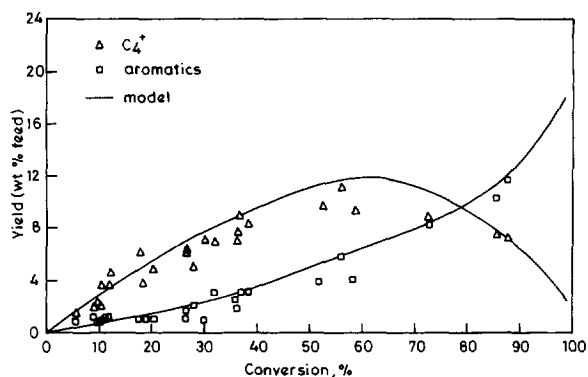


Fig. 9. Comparison between predicted and experimental yields of  $C_4^+$  and aromatics.

$C_2H_4$  and 1,3- $C_4H_6$  are in agreement up to a conversion of 60–70%, while at higher conversions the calculated yields are somewhat higher than the experimental values. The calculated yields of  $C_4^+$  and 1,3- $C_4H_6$  showed maxima at 60.0% and 90.0% conversion, respectively, whereas experimentally the maxima in  $C_4^+$  yields were obtained at 56.0% conversion and for 1,3- $C_4H_6$  at 81.5% conversion (Figs. 8 and 9).

The sensitivity of the model was checked by increasing the rate constants of each of the reactions by 10%. The calculated yields were significantly affected by changing the rate constant of the primary reaction as well as by the rates of reaction (10), (11), (23) and (24) of Table 2. However, there was

only a minor change in the product yields when the rates of the other secondary reactions were varied.

## 5. Conclusions

Based on the results of this study, it can be concluded that, in the temperature range of 953–1073 K, the overall decomposition reaction of methylcyclohexane can be represented by an approximate first-order reaction with an activation energy of 209  $\text{kJ mol}^{-1}$ . The major products are methane, ethylene, propylene and 1,3-butadiene, and cyclohexene, methylcyclohexenes, isoprene, benzene and toluene are also formed in appreciable amounts. The experimental product yields can be satisfactorily simulated using a molecular model consisting of a primary reaction and 24 secondary reactions.

## Acknowledgements

The financial support provided by the Department of Science and Technology, New Delhi, for this study is gratefully acknowledged.

## References

- [1] M. Bajus, V. Vesely, P.A. Leclercq, J.A. Rijks, *Ind. Eng. Chem. Prod. Res. Dev.* 18 (1979) 135.
- [2] R. Mukhopadhyay, D. Kunzru, *Ind. Eng. Chem. Res.* 32 (1993) 1914.
- [3] B. Basu, D. Kunzru, *Ind. Eng. Chem. Res.* 31 (1992) 146.
- [4] P.S. van Damme, G.F. Froment, W.B. Balthasar, *Ind. Eng. Chem. Process Des. Dev.* 20 (1981) 366.
- [5] P. Kumar, D. Kunzru, *Ind. Eng. Chem. Process Des. Dev.* 24 (1985) 774.
- [6] F. Billaud, M. Duret, K. Elyahyaoui, F. Baronnet, *Ind. Eng. Chem. Res.* 30 (1991) 1469.
- [7] D.S. Aribike, A.A. Susu, A.F. Ogunye, *Thermochim. Acta* 51 (1981) 113.
- [8] K.K. Pant, D. Kunzru, *J. Anal. Appl. Pyrol.* 36 (1996) 103.
- [9] W. Tsang, *J. Phys. Chem.* 76 (1972) 143.
- [10] K.H. Ebert, H.J. Ederer, G. Isbarn, *Int. J. Chem. Kinet.* 15 (1983) 475.
- [11] F. Billaud, K. Elyahyaoui, F. Baronnet, *Chem. Eng. Sci.*, 46 (1991) 2941.
- [12] M. Murata, S. Saito, *J. Chem. Eng. Jpn.* 8 (1975) 39.
- [13] K.M. Sundaram, G.F. Froment, *Chem. Eng. Sci.* 32 (1977a) 601.
- [14] K.M. Sundaram, G.F. Froment, *Chem. Eng. Sci.* 32 (1977b) 609.
- [15] R. Zou, Q. Lou, S. Mo, S. Feng, *Ind. Eng. Chem. Res.* 32 (1993) 843.
- [16] L.P. Hillewaert, J.L. Dicrickx, *AIChE J.* 34 (1988) 17.